Mon. Not. R. astr. Soc. (1990) **245**, 71–81

A search for quasars in a field around NGC 520★

E. Gosset,[1] R. G. Clowes,[2] J. Surdej[3]† and J. P. Swings[3]

[1] *European Southern Observatory, Karl-Schwarzschild-Str. 2, D-8046 Garching bei München, FRG*
[2] *Royal Observatory, Blackford Hill, Edinburgh EH9 3HJ, Scotland*
[3] *Institut d'Astrophysique, Université de Liège, avenue de Cointe 5, B-4200 Cointe-Ougrée, Belgium*

Accepted 1990 January 31. Received 1989 December 13; in original form 1989 April 6

SUMMARY

We have performed an objective-prism search for quasars in a field around the galaxy NGC 520. The AUTOMATED QUASAR DETECTION (AQD) software has been applied and a sample of 175 highly rated quasar candidates has been selected and is presented here. The 2D and 3D distributions of the candidates have been analysed. The distribution on the celestial sphere turns out to be non-random. The deviations from randomness are both a tendency to exhibit anticorrelation at the scale of a few arcmin and a significant excess of objects at separations of about 20 arcmin. A very weak tendency towards spatial clustering is also detected (significance level 0.04) at a typical scale of 10 h^{-1} Mpc, but it concerns an extremely small number of candidates and a definitive conclusion is delayed until all the candidates have been observed spectroscopically. Finally, in order to test the claims by Arp & Duhalde that an excess of quasars exists near NGC 520 and that there is a preferential NE–SW alignment of bright quasars across this amorphous galaxy, we have also performed various statistical analyses of the distribution of the high-grade quasar candidates with respect to NGC 520: no sign of any possible relation is present in our data.

1 INTRODUCTION

Several partially overlapping fields ($\sim 5° \times 5°$) near and far from selected bright galaxies (NGC 5334, 450, 520, etc.) have been searched for quasar candidates on the basis of the presence of an ultraviolet excess ($U-B \lesssim -0.4$). This work was initiated several years ago (Arp & Surdej 1982; Surdej *et al.* 1982) and the most recent status reports may be found in Gosset, Surdej & Swings (1986) and in Swings, Surdej & Gosset (1988). Initially, this project was triggered by the need for further observational evidence supporting the uniform distribution of quasars, their possible location in superclusters (Oort 1981; Oort, Arp & de Ruiter 1981; Oort 1983), or near bright galaxies and/or their companions (Arp 1981; Arp 1983). The particular field of NGC 520 is of importance since several anomalies have been claimed concerning the distribution of quasars with respect to NGC 520 itself (local overdensity, alignment across the galaxy; see Arp & Duhalde 1985). In addition, it became clear that the analysis of the distribution of quasars was interesting *per se*, since an extensive study should lead to a better understanding of some general characteristics of the Universe (distribution and physical properties of matter at large scales, etc.). It therefore appeared important to select and study large areas of the sky with as high a degree of completeness as possible. It is for this very precise reason that we decided to search for quasars in the same area near NGC 520 as Swings *et al.* (1988) had done, although using a different technique: namely the detection of quasar candidates by means of objective-prism plates.

Since this addresses, at least partially, a different population of quasars from the one selected on the basis of the U/B excess, the use of somewhat complementary searches should also help in evaluating the completeness of the different surveys. Furthermore, the combination of different samples of quasar candidates derived from the same field should enable one to disentangle the possible effects due to observational biases against inherent physical properties of the Universe constituents. For instance, assembling together U/B excess and emission-line quasar candidates should prove useful in order to check whether the recent claims of evolution of the clustering properties of quasars with redshift (Iovino & Shaver 1988; Kruszewski 1988, 1990) are relevant or are due to observational biases. Indeed, the studies mentioned above are based either on heterogeneous data from large catalogues, or on composite samples of quasars.

This paper deals with the study of the first field, around NGC 520, for which the objective-prism plate search for quasar candidates has been achieved; the selection has been

★ Based on observations collected with both the UK 1.2-m and ESO 1.0-m Schmidt telescopes.
†Also, chercheur qualifié au Fonds National de la Recherche Scientifique (Belgium).

made using the AQD (Clowes 1986a, b, 1988) software developed in Edinburgh. While searching objective-prism plates by eye has proven to be a successful method (Clowes & Savage 1983), it is now established that the homogeneity and the consistency of a survey can be markedly improved by using the recently available automated techniques.

In Section 2, we give details on the selection of the quasar candidates and present the resulting sample. A study of the 2D (on the celestial sphere) and 3D distributions of the candidates is addressed in Section 3. Such a study is in no way intended to give a definitive answer to the problem of quasar clustering, but we consider it useful to get a deep insight into the properties of this new sample. Section 4 contains the analysis of the relative positions of the quasar candidates with respect to NGC 520.

2 OBSERVATIONS AND SELECTION OF THE QUASAR CANDIDATES

Two plates have been acquired in order to complete the first part of the survey reported here. The first one is a direct plate of the field. None being available in the UKSTU (United Kingdom Schmidt Telescope Unit) archive, one such plate (ESO5723A, see Table 1) was taken with the ESO Schmidt Telescope at the European Southern Observatory (La Silla, Chile).

Plate ESO5723A was scanned in the image analysis mode (IAM) of the COSMOS measuring machine in Edinburgh (MacGillivray & Stobie 1984). The nominal spot size and the pixel size were set to 16 μm and the transmission scale had 256 digitization levels. The number of catalogued images was 46 670: the star/galaxy classification (MacGillivray & Stobie 1984) was possible for 37 246 of them. The bad seeing conditions prevailing during the observation meant that the star/galaxy classification was much poorer than usual, however.

Images separated by less than ± 70 pixels in the x-direction (dispersion direction) and ± 3 pixels in the y-direction were classified as geometric overlaps, having 'geometrically overlapped' spectra on the objective-prism plate (see below). These objects are routinely excluded from further treatments since they would mimic quasar-like features. Seven thousand four hundred and seventeen objects of the 46 670 images turned out to be in this category.

The (α, δ) positions of the images were iteratively calibrated on the basis of some 100 catalogue stars well distributed over the whole plate. The accuracy of the celestial coordinates is determined by the catalogue and is of the order of 1 arcsec over the entire area.

The second photographic plate is an objective-prism one that was obtained with the UK Schmidt Telescope in Australia. This plate, UJ7308P, exposed under relatively good seeing conditions was taken on hypersensitized Kodak IIIa-J emulsion. More details are given in Table 1. Plate UJ7308P was scanned by COSMOS in the mapping mode (MM). The sky background level on this plate was high, leading to significant machine-introduced noise; this problem was overcome by measuring a glass copy (UJ7308P P1 N1) of the original plate.

Table 1. Details on the direct plate ESO5723A and on the objective-prism plate UJ7308P.

Plate	ESO direct	UKST objective-prism
Plate number	ESO5723A	UJ7308P
Field	around NGC 520	around NGC 520
Field centre	$\alpha(1950) = 01^h\ 19^m\ 14^s$	$\alpha(1950) = 01^h\ 18^m\ 12^s$
	$\delta(1950) = 04°\ 49'\ 41''$	$\delta(1950) = 04°\ 49'\ 08''$
Field scale	5° × 5°	6°.4 × 6°.4
Emulsion	IIa-O	IIIa-J
Hypersensitization*	None	27N + 6H + 4
Exposure time	25 min.	70 min.
Date	1984 July 27/28	1981 October 28/29
Effective seeing	3-4 arcsec.	2 arcsec.
Telescope	ESO 1.0m Schmidt	UK 1.2m Schmidt (Australia)
Filter	B (GG385)	–
Prism	–	44 arcmin.
Nominal dispersion	–	2400 Å mm^{-1} at 4300 Å
Dispersion direction	–	N–S
Plate scale	67.5 arcsec. mm^{-1}	67.12 arcsec. mm^{-1}

* See Clowes & Savage (1983).

Table 2. Details on the selection limits and the detection rates (see Clowes 1986a, and references therein).

Selection limits:

Emission:	Limit of line criterion:	6.0	
	Limit of continuum criterion:	1.0	
Ultraviolet excess:	Filter 1:	46	61 (pixels)
		3815	3486 (Å)
	Filter 2:	22	34 (pixels)
		4659	4170 (Å)
	Colour limit:	0.45	

Detection rates:

	Star-like	Galaxy-like	Unclassified
Emission	827	89	21
Ultraviolet excess	538	92	47
Both	100	14	3

Software developed at ROE was then used to map the direct plate coordinates to the objective-prism plate coordinates using an upgraded version of the method described by Clowes (1986a). Spectra in the form of 128×8 16-μm pixels were extracted for all images detected on plate ESO5723A. The AQD software (Clowes 1986a, b, 1988, and references therein) was utilized to construct from each image a 1D spectrum and to analyse it in order to search for spectral features that are characteristic of quasars. The AQD quality testing rejected more than half of the spectra because they were too faint, saturated or otherwise flawed; faintness was of course the main rejection reason as the direct plate is much deeper than the objective-prism one. One thousand four hundred and ninety seven objects were finally selected on the basis of the presence of at least one emission line or of an ultraviolet excess. A great part of the former selections result from a stellar feature that can mimic emission lines (see Section 3.2 for more details). Table 2 presents quantitative details of the selection criteria and information about the partition of the provisional candidates into different classes of selection.

Following a new procedure (Clowes, Iovino & Shaver 1987), points were awarded to each object of this first sample in a grading scheme, in order to select a subsample of high-grade quasar candidates. One hundred and seventy five objects have been selected in this way. From visual prejudice, they are estimated to be quasars at the minimal 60 per cent (± 5 per cent) probability level. They are listed in Table 3. The grading scheme is such that all the high-grade candidates satisfy, at least, the emission-line criterion. The limiting magnitude is estimated to be about 19.5; a better estimate as well as individual magnitudes for the quasar candidates will be derived once the photometric sequences (Swings *et al.* 1988) are fully reduced.

Table 3. Positions of the high-grade quasar candidates.

	α(1950)			δ(1950)		
1	01^h	09^m	$49\overset{s}{.}7$	03°	35′	12″
2	01	09	55.1	05	33	33
3	01	10	02.7	06	40	11
4	01	10	08.0	04	14	27
5	01	10	14.7	04	51	31
6	01	10	23.3	03	17	48
7	01	10	24.8	03	09	40
8	01	10	26.3	05	59	29
9	01	10	29.1	06	48	50
10	01	10	36.5	04	56	29
11	01	10	37.3	04	00	47
12	01	10	44.5	06	30	34
13	01	10	44.8	06	55	42
14	01	11	03.6	05	54	34
15	01	11	07.0	03	17	41
16	01	11	14.6	05	27	41
17	01	11	29.2	06	53	53
18	01	11	32.2	05	30	24
19	01	11	36.4	03	06	00
20	01	11	52.0	05	11	30
21	01	11	52.7	05	12	16
22	01	11	57.9	04	30	10
23	01	11	58.5	02	18	46
24	01	12	18.3	02	59	06
25	01	12	23.5	06	18	22
26	01	12	25.6	03	18	35
27	01	12	39.0	06	55	51
28	01	12	41.9	03	40	11
29	01	13	06.9	02	56	04
30	01	13	12.6	02	30	20
31	01	13	14.0	03	51	33
32	01	13	20.6	03	17	52
33	01	13	22.6	04	59	30
34	01	13	23.7	02	20	06
35	01	13	41.3	06	50	37
36	01	13	45.0	03	39	52
37	01	13	50.2	05	48	26
38	01	13	55.7	06	21	42
39	01	14	00.8	02	42	44
40	01	14	01.9	06	39	04
41	01	14	10.5	05	09	25
42	01	14	17.0	04	10	49
43	01	14	18.2	02	28	56
44	01	14	32.3	04	10	28
45	01	14	44.4	02	34	43
46	01	14	47.3	06	23	10
47	01	14	48.9	02	31	57
48	01	15	18.0	03	33	49

Table 3. – *continued*

	α(1950)			δ(1950)		
49	01^h	15^m	$21^s.8$	07°	11′	28″
50	01	15	21.9	05	14	03
51	01	15	25.5	07	10	15
52	01	15	39.0	03	04	48
53	01	15	39.4	04	51	28
54	01	15	47.6	06	07	11
55	01	15	54.1	02	53	08
56	01	15	54.4	04	32	15
57	01	15	56.3	06	30	40
58	01	15	56.9	06	23	18
59	01	16	01.7	05	06	03
60	01	16	06.1	05	19	07
61	01	16	06.4	05	23	38
62	01	16	07.1	05	08	50
63	01	16	09.6	05	52	41
64	01	16	21.1	04	48	59
65	01	16	23.8	06	47	01
66	01	16	29.0	03	09	47
67	01	16	39.2	03	57	42
68	01	16	48.2	02	51	00
69	01	16	49.3	05	11	04
70	01	17	09.8	03	49	15
71	01	17	11.9	05	12	23
72	01	17	17.6	03	23	09
73	01	17	19.7	05	35	44
74	01	17	23.1	04	56	36
75	01	17	31.4	07	07	24
76	01	17	35.2	05	10	06
77	01	18	11.0	04	25	24
78	01	18	31.1	05	36	00
79	01	18	34.8	05	42	57
80	01	18	48.6	02	44	12
81	01	19	00.7	03	32	09
82	01	19	34.8	03	10	04
83	01	19	36.1	04	08	36
84	01	19	58.7	03	20	58
85	01	20	01.3	06	53	32
86	01	20	05.6	05	00	51
87	01	20	22.3	02	29	02
88	01	20	28.4	03	13	21
89	01	20	29.2	06	15	09
90	01	20	34.2	03	58	40
91	01	20	35.1	05	39	36
92	01	21	02.6	07	12	40
93	01	21	12.4	04	41	52
94	01	21	14.5	04	30	43
95	01	21	17.6	04	56	42
96	01	21	19.2	06	20	42

Table 3. – *continued*

	α(1950)			δ(1950)		
97	01^h	21^m	$21^s.7$	06°	24′	25″
98	01	21	25.7	05	59	39
99	01	21	27.3	03	54	14
100	01	21	32.9	05	53	20
101	01	21	39.6	07	13	55
102	01	21	43.0	03	26	59
103	01	21	47.3	02	28	32
104	01	21	48.3	05	40	36
105	01	21	52.5	04	58	37
106	01	22	02.1	06	10	20
107	01	22	09.4	03	05	49
108	01	22	14.0	06	14	07
109	01	22	21.3	05	49	37
110	01	22	22.3	03	38	12
111	01	22	25.0	06	23	01
112	01	22	38.2	03	51	07
113	01	22	39.0	04	46	35
114	01	22	39.9	05	11	23
115	01	22	51.4	06	15	14
116	01	22	51.4	04	32	45
117	01	23	03.5	06	22	32
118	01	23	09.8	06	58	05
119	01	23	20.8	06	59	14
120	01	23	33.3	07	15	06
121	01	23	46.1	04	41	52
122	01	23	47.2	06	20	21
123	01	23	48.6	06	59	12
124	01	23	59.0	03	09	03
125	01	24	00.5	06	36	15
126	01	24	01.1	04	34	20
127	01	24	12.2	05	12	29
128	01	24	18.5	06	52	05
129	01	24	30.5	06	17	50
130	01	24	31.1	05	59	30
131	01	24	32.1	04	01	51
132	01	24	34.9	05	03	22
133	01	24	42.8	05	25	51
134	01	24	52.1	07	03	19
135	01	24	58.7	06	16	13
136	01	25	01.3	04	54	41
137	01	25	08.2	02	33	46
138	01	25	21.6	05	35	07
139	01	25	25.1	04	52	25
140	01	25	34.0	03	42	37
141	01	25	38.8	02	57	39
142	01	25	44.8	06	32	01
143	01	25	45.5	04	04	33
144	01	25	47.4	03	38	05

Table 3. – *continued*

	α(1950)			δ(1950)		
145	01^h	25^m	$51^s.0$	03°	25′	38″
146	01	25	59.9	03	48	43
147	01	26	00.8	04	50	29
148	01	26	00.8	02	29	41
149	01	26	04.6	03	04	12
150	01	26	06.8	03	18	01
151	01	26	13.1	04	37	14
152	01	26	23.5	04	07	40
153	01	26	29.8	06	18	17
154	01	26	38.8	04	12	03
155	01	26	50.3	04	48	30
156	01	26	58.6	03	16	57
157	01	27	04.7	02	31	07
158	01	27	04.8	03	51	34
159	01	27	07.8	06	35	34
160	01	27	08.5	03	32	42
161	01	27	12.3	07	09	04
162	01	27	17.7	04	33	42
163	01	27	21.2	06	45	10
164	01	27	25.9	05	10	23
165	01	27	57.8	05	46	25
166	01	28	08.7	03	34	02
167	01	28	09.4	04	08	31
168	01	28	24.5	06	57	30
169	01	28	49.3	03	51	02
170	01	28	49.9	06	58	57
171	01	29	09.4	07	00	30
172	01	29	39.5	03	15	04
173	01	29	41.5	04	17	49
174	01	29	46.2	05	33	25
175	01	29	48.4	04	32	47

3 THE 2D AND 3D DISTRIBUTIONS OF THE QUASAR CANDIDATES

3.1 The 2D case

The 175 quasar candidates were projected on a plane (5°×5°) using Webster's (1976b) method of equal area projection. Then, they were submitted to a detailed analysis of their 2D distribution. The adopted null-hypothesis is one which states uniformity, independency and randomness (Webster 1976a). As pointed out by Gosset, Surdej & Swings (1988), it is worth using several fundamentally different methods to analyse a distribution of points. Effectively, each method has its own advantages, sensitivity, and properties but also has its defects and weaknesses. Without doubt, the combined results of several independent methods are essential to reach a high degree of confidence in the conclusions of the analysis. We have searched the literature in order to assemble good methods; we have retained a set of five of them for their fundamentally different natures. The first four are the multiple binning analysis (MBA), the power spectrum analysis (PSA), the nearest neighbours analysis (NNA) and the correlation function analysis (CFA). They permit the analysis of the sample at different scales but share the common defect of not being suitable for analysing the data at a typical scale of the order of that of the whole field. Fortunately, this is not the case of the well-known 1D Kolmogorov–Smirnov test. As a consequence, this test is complementary to the other methods and could be thought of as a fifth method to be applied. Peacock (1983) has proposed an extended Kolmogorov–Smirnov (EKS) test for the 2D case while, recently, Gosset (1987a) has introduced the 3D EKS test. We refer the reader to Gosset (1987b) for a comprehensive description and a critical study of the various statistics used as well as for a detailed comparison between the five different tests. A brief account can also be found in Gosset *et al.* (1988). Hereafter, the results from each test applied are briefly outlined and a general summary is given in Table 4. The notations are the standard ones (Gosset 1987b). Since our experience in the field, based on numerous applications and simulations, suggests that the CFA could be the most powerful test despite its great sensitivity to biases, we will give some details on the results of this particular application.

The 2D EKS test yields a value of the statistic $Z^{(2)}_{175}$ (see Table 4) that denotes the absence of any large-scale deviation from uniformity. The second test, the MBA applied in the framework of the 4 within 16 randomization test (Gosset & Louis 1986), reveals two marginal deviations from randomness for the relevant normal Z-statistic. The first one corresponds to a typical scale of 1/256 of the length of one side of the field, i.e. about 1.2 arcmin. The normal Z-statistic reaches a value of $+2$, corresponding to a tendency to cluster with a significance level of 0.022; however, at such a scale, the bins are not well populated. The second deviation leads to $Z=-1.67$, is directed towards regularity (e.g. like a lattice) and exhibits a significance level of 0.047 at a scale of about 1/16 of the side length, i.e. about 20 arcmin.

As the EKS and the MBA detect no deviation at large scale (~ that of the field), it is safe (Peacock 1983) to apply the PSA as a third test. The run of the Q'-statistic has been investigated in the range $1/\lambda \sim 0.5$ to 200 degree^{-1}. Nothing significant has been noticed except for the presence of two peaks at $1/\lambda = 49.3$ degree^{-1}(1.2 arcmin) and at $1/\lambda = 163.9$ degree^{-1}(22 arcsec) (see Table 4). Both correspond to tendencies towards regularity, which is in disagreement with the results from the MBA. The Q-statistic suggests that no clustering is present.

The fourth test, the NNA, detects no deviation from randomness: the mean observed distance to the nth nearest neighbour ($n=1\rightarrow15$) agrees always within 1.5 standard deviations with the theoretically expected value. It must be pointed out that the mean distance to the nearest neighbour is roughly 0°.19 (11–12 arcmin) and that the two peaks exhibited by the PSA are far beyond this limit. Some caution is therefore necessary.

Application of the CFA consists in estimating the covariance function of the sample by making counts in concentric rings sequentially built-up around each object (Fall 1979). This method is extremely sensitive to edge effects (i.e. some parts of the concentric rings are in regions outside the field) and a correction has therefore to be applied. The only

Table 4. Summary of the results (statistics, angular or linear scales, significance levels, comments) obtained from the application of various statistical tests (see the references) to the distribution of the high-grade quasar candidates.

A. The 2D case

Test	Statistics	Scale	SL	Comments
EKS	$Z^{(2)}_{175} = 1.23$			Absence of any large scale deviation
(1)(2)	$(Z^{(2)}_{\infty} = 1.24)$			from uniformity
MBA	$Z = 2.00$	1.'2	0.022	Tendency towards clustering
(3)	$Z = -1.67$	20′	0.047	Tendency towards regularity
PSA	$Q' = 1.039 \pm 0.016$	1.'2	0.008	Tendency towards regularity
(4)(5)(6)	$Q' = 1.022 \pm 0.009$	22″	0.006	Tendency towards regularity
NNA				Absence of any deviation from
(5)				randomness
CFA	$w_{data/data} = 0.23$	$\sim 20'$	see Fig.1	Overdensity of objects
(7)(8)(5)	$w_{data/data} = -0.33$	$< 5'$	see Fig.1	Anticorrelation

B. The 3D case

Test	Statistics	Scale	SL	Comments
EKS	$Z^{(3)}_{123} = 2.36$	$\gtrsim 200\ h^{-1}$Mpc	0.01	Detection of non-uniformity at large
(2)	$(Z^{(3)}_{\infty} = 2.38)$			scale
GPSA				No other deviation from uniformity
(1)(5)				
MBA	$Z = 1.75$	$9\ h^{-1}$Mpc	0.040	Tendency towards clustering
(3)	$Z \gtrsim 2.4$	$> 50\ h^{-1}$Mpc	0.009	Non-uniformity at large scale
NNA	$R^{(3)}_1 = 0.94$		0.040	Tendency to form pairs
(5)				
CFA	$w_{data/data} = 4.8$	$< 5\ h^{-1}$Mpc	~ 0.040	Tendency towards clustering
(7)(8)(5)	$w_{data/data} = 1.7$	5-10 h^{-1}Mpc	see Fig.3	

(1) Peacock (1983)
(2) Gosset (1987a)
(3) Gosset & Louis (1986)
(4) Webster (1976a)
(5) Gosset (1987b)
(6) Gosset, Surdej & Swings (1988)
(7) Fall (1979)
(8) Sharp (1979)

way to perform this correction properly is to calculate the exact measure of the domain actually explored when making the counts and to scale the latter ones accordingly (Gosset 1987b). Unfortunately, the secondary effect of this approach is twofold. First, systematic effects could be induced, in particular if the sample presents large-scale ($\sim$ that of the field) inhomogeneities. Secondly, some additional redundancy is introduced in the counts. This implies a change in the dispersion of the statistic built from these counts. The best way to take these effects into account has been suggested by Sharp (1979) and consists nowadays of computing the mean cross-covariance function between simulated populations of (usually) uniformly distributed individuals (representing the null-hypothesis) and the data. Two estimators of the cross-covariance function can be defined: one for which the concentric rings are built-up around the simulated individuals and the counts are performed on the data; the other one for which the reverse is done. This will lead to two functions, denoted respectively $w_{\mathrm{random/data}}$ and $w_{\mathrm{data/random}}$. The systematic biases possibly present in $w_{\mathrm{data/data}}$ (the autocovariance) are isolated by $w_{\mathrm{random/data}}$. Therefore, the actual autocovariance can be estimated from the comparison of $w_{\mathrm{data/data}}$ with $w_{\mathrm{random/data}}$. The advantage of this technique is important: there is no need for a model of the possible large-scale inhomogeneity and, therefore, no *a priori* decision has to be made. In addition, the function $w_{\mathrm{data/random}}$ is unbiased

and its dispersion over the simulations is a convenient estimate of the uncertainty (Sharp 1979; Gosset 1987b). The results from the CFA are shown in Fig. 1 where we have plotted the functions $w_{\text{data/data}}$ (autocovariance of the data) and $w_{\text{random/data}}$; the error bars represent $\pm$one standard deviation, over the simulations, in the distribution of the function $w_{\text{data/random}}$ (i.e. under the null-hypothesis). Only one point deviates by more than three standard deviations. It corresponds to the bin $\theta \in [0\overset{\circ}{.}25, 0\overset{\circ}{.}33]$ whose associated scale is 20 arcmin. This deviation points towards an overdensity of objects at this separation and agrees well with the regularity detected by the MBA. Although the PSA does not give any confirmation, the effect seems real since it is outlined by two different methods. Another interesting feature is the anticorrelation seen in the first bins. The very first one, in particular, reaches a value $w(\theta) = -0.33$. It is tempting to connect this result with the regularity at 1.2 arcmin suggested by the PSA and to notice that out of the 46 670 catalogued objects on the direct plate, 7417 have been rejected due to a geometric overlap of their spectrum with neighbouring ones. Out of the 39 253 remaining objects, we have selected 175 high-grade quasar candidates in order to constitute the second sample. It is reasonable to think that, in addition to these 175 quasar candidates, some 33 candidates (roughly $175 \times 7417/39\,253$) would have been selected but have been discarded very early in the process due to their classification as overlaps. It is usually admitted that these objects are spatially randomly distributed. This is true, at least approximately, if we consider their location within the field, but this is clearly incorrect if we consider their relative position with respect to other objects. A length of 70 pixels corresponds roughly to $0\overset{\circ}{.}02$ (i.e. ~ 1.2 arcmin) and any pair with such a small separation has a greater probability of being discarded. If our considerations are true, the effect must be visible in the first sample constituted by the 1497 provisional quasar candidates. The present interest of this sample is that the larger number of objects it contains will allow a better resolved binning of the CFA. Consequently, we have computed the relevant autocovariance of the first sample and found that, indeed, only the first bin ($\theta \leq 0\overset{\circ}{.}02$) presents a deviation from randomness in the region of interest; w adopts a value of -0.19 there. As a consequence, we may state that the automatic removal of overlapping spectra creates an effect which is easily detected in the sample of 1497 provisional quasar candidates. As an appreciable number of close pairs is discarded, the PSA will usually detect the associated regularity at a scale around 1.2 arcmin, even in smaller samples (as could be the case here for the sample of 175 high-grade quasar candidates). When the size of the sample is too much decreased, however, the density does the same and it becomes less likely to have such close pairs initially. Concerning the case of the sample of 175 high-grade quasar-candidates, this means that all the 33 candidates that have been discarded due to their classification as overlaps, were most probably forming pairs with non-candidates. Therefore, their disappearance is not affecting the first bins of the CFA predominantly. In the present context, a value of the statistic (for $\theta \leq 5$ arcmin) lower than -0.10 cannot be attained by the sole act of removing all pairs closer than 1.2 arcmin from an hypothetical unvitiated high-grade sample. Therefore, the value $w(\theta \leq 0\overset{\circ}{.}083) = -0.33$ essentially pertains to the data and the relevant tendency towards anticorrelation is not an artefact.

The main conclusion of these studies may be summarized as follows: the distribution on the celestial sphere of the 175 high-grade quasar candidates departs from randomness. The main deviations consist of a tendency towards anticorrelation at angular scales of a few arcminutes and of an overdensity of objects at separations of about 20 arcminutes.

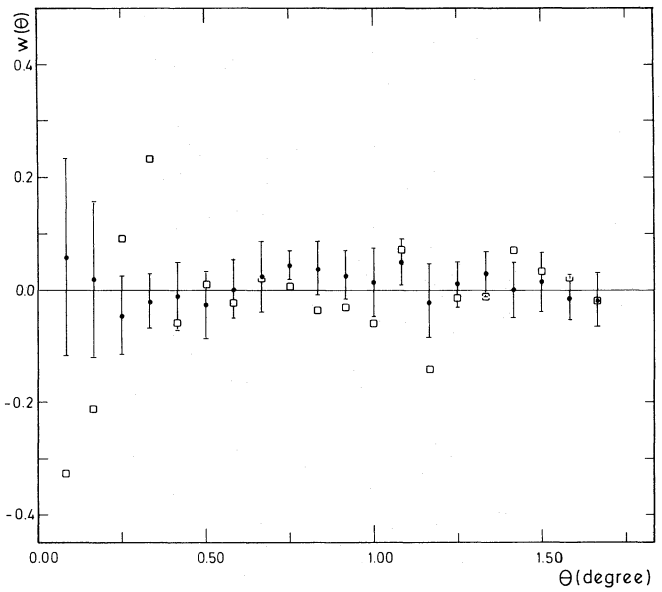

Figure 1. Run of the $w(\theta)$ statistic for the 2D CFA applied to the sample of 175 high-grade quasar candidates. The squares represent the function $w_{\text{data/data}}$, the points the function $w_{\text{random/data}}$. Error bars are ± 1 standard deviation as computed from the dispersion on the function $w_{\text{data/random}}$. The abscissa represents the angular scale expressed in degrees.

3.2 The 3D case

In order to complete this preliminary study, we decided to analyse the 3D distribution of the high-grade quasar candidates. Redshifts for the quasar candidates were thus needed: they have been estimated on the basis of the low-dispersion spectra extracted from the objective-prism plate. Such estimates are subject to both systematic and random errors ($\sigma_z \sim 0.015$–0.020), and are based on the assumption that the detected emission line is Lyα. In addition, it should be pointed out that the redshift scale is discrete ($\Delta z \sim 0.02$). All the 175 high-grade candidates display a sufficiently useful spectrum to allow a trial redshift value to be derived for each of them: the resulting provisional redshifts lie in the range [1.8, 3.1], with a peak (23 per cent) between 2.2 and 2.3. Such an excess could indicate that part of the sample is still contaminated by stars or galaxies. It is well known (Drinkwater 1986) that the combination of the 4000 Å break and of the *G*-band (4300 Å) absorption may mimic the presence of an emission line. As usual, we have removed routinely all objects with a redshift greater than 2.4 from the sample since they could induce a distortion of the scales and in addition their redshifts carry larger errors.

This third sample contains 123 objects. They have been put in a parallelepiped within a euclidean space ($q_0 = 1/2$). The small range of redshift permits the whole parallelepiped

to be filled with the explored volume. For example, we can compute the x and y positions (perpendicular to the line-of-sight) by multiplying the projected angular position of each object, as computed in Section 3.1, by the mean distance of the sample whereas the position along the third axis is obtained by the trivial conversion of the redshift into a distance. The dimensions of the resulting volume are $0.24 \times 0.24 \times 0.4$ h^{-3} Gpc^3 (where the present Hubble constant is taken to be $H_0 = h\,100$ km s^{-1} Mpc^{-1}).

The results obtained from the application of the different tests are summarized in Table 4. The MBA detects large-scale ($> 50\ h^{-1}$ Mpc) inhomogeneities, a result confirmed by the EKS test which strongly rejects the null-hypothesis of uniformity. The particular distribution of the redshifts is certainly responsible for this. We have analytically modelled this distribution, and again applied the EKS test with the newly derived cumulative distribution function. The rejection is less well marked but the effect is still present with a significance level of 0.01, which remains important.

The existence of a large-scale inhomogeneity (be it physical or not) implies that we cannot apply the PSA: we are thus led to use the GPSA (generalized power spectrum analysis; Peacock 1983). In addition, the density of quasar candidates in the volume being extremely low, this prevents us from securely applying the 3D GPSA. In any case, a straightforward application of this method leads to the non-detection of any anomaly.

The CFA has also been applied and the result is shown in Fig. 2. The first bin indicates a marked clustering and the second one presents, to some extent, the same behaviour. One also sees that $w_{\mathrm{data/data}}$ systematically keeps positive values for the whole range of characteristic lengths investigated. The statistic $w_{\mathrm{random/data}}$ does not show this effect. Clearly, we have to deal with the manifestation of the large-scale inhomogeneity detected by the EKS and MBA tests (see Table 4). We can include this large-scale inhomogeneity in the null-hypothesis: we only have to modify accordingly the characteristics of the *random* populations. Instead of considering uniform populations, we shall now generate the *random* populations by randomizing the redshifts over the different objects. Such an approach has the advantage of perfectly reproducing (of course) the observed distribution of redshifts and of taking into account the discrete nature of the redshift scale. The main disadvantage is that the new resulting null-hypothesis is always more reminiscent of the data than the old one, which renders the test conservative. The result is shown in Fig. 3. Clearly, in this case, the function $w_{\mathrm{random/data}}$ accounts perfectly well for the systematic behaviour of $w_{\mathrm{data/data}}$. The only remaining deviations concern the two first bins and tend to indicate a clustering. The first bin, in particular, is at more than two standard deviations from the expectation, which roughly corresponds to a significance level of 0.040. The test is now effectively more conservative. The tendency towards clustering is confirmed, at the same significance level, by the MBA and NNA tests (see Table 4).

These results are mainly indicative of the characteristics of the sample. It is well known that a single field is subject to large statistical fluctuations (see e.g. the detected clustering in the field of plate UJ3682P; Drinkwater 1988). The tendency towards clustering reported here above pertains to the data, but the significance level is still too large to permit any attribution of the characteristic to the parent population of quasars. As stated above, we are not able to get a definitive answer about the problem of quasar clustering on the basis of

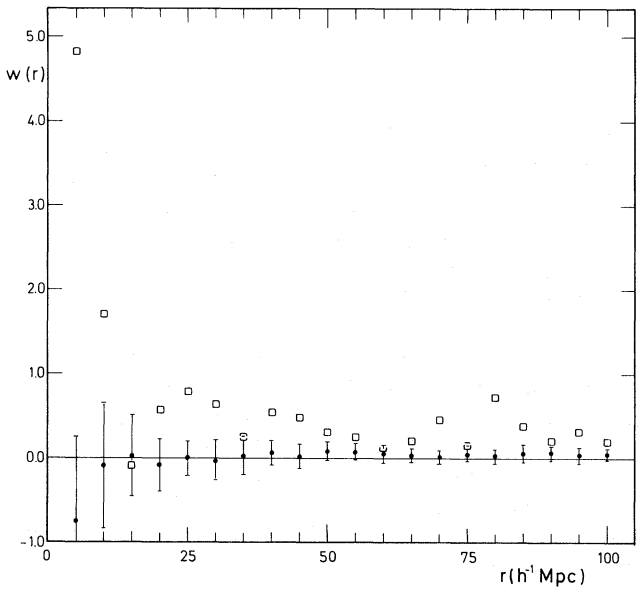

Figure 2. Run of the $w(r)$ statistic for the 3D CFA applied to the sample of 123 high-grade quasar candidates with provisional redshifts between 1.8 and 2.4. The squares represent the function $w_{\mathrm{data/data}}$, the points the function $w_{\mathrm{random/data}}$. Error bars are ± 1 standard deviation as computed from the dispersion on the function $w_{\mathrm{data/random}}$. The abscissa represents the spatial scale expressed in h^{-1} Mpc.

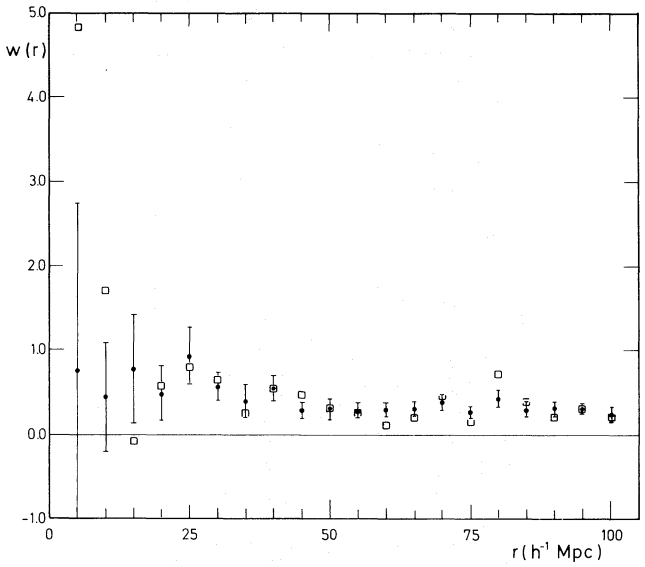

Figure 3. Run of the $w(r)$ statistic for the 3D CFA applied to the sample of 123 high-grade quasar candidates with provisional redshifts between 1.8 and 2.4. The squares represent the function $w_{\mathrm{data/data}}$, the points the function $w_{\mathrm{random/data}}$. Error bars are ± 1 standard deviation as computed from the dispersion on the function $w_{\mathrm{data/random}}$. *Random* here means that the simulated populations have been obtained by randomizing the redshifts among the quasar candidates. The abscissa represents the spatial scale expressed in h^{-1} Mpc.

the present sample alone. Nevertheless, it is interesting to compare our results to other ones reporting a positive detection of clustering. The most recent results are referenced and discussed in Shanks, Boyle & Peterson (1988): these authors find, for separations less than the canonical value 10 h^{-1} Mpc, a 'correlation' function $\xi = 1.25$ for their whole redshift range $0.3 \leq z \leq 2.2$ and $\xi = 1.00$ for the redshift range $1.4 \leq z \leq 2.2$. Referring to the same scale, we find $w_{\mathrm{data/data}} = 2.03$ and $w_{\mathrm{random/data}} = 0.49$. We can estimate the equivalent 'correlation' function using the following expression

$$\xi \sim \frac{w_{\mathrm{data/data}} - w_{\mathrm{random/data}}}{1 + w_{\mathrm{random/data}}} \sim 1.04.$$

The latter value is in good agreement with the conclusions of Shanks *et al.* (1988), although the redshift ranges are somewhat different. The more extensive quasar sample of Shanks *et al.* (1988) induces an ability to reject the null-hypothesis (about 4.2σ) which is not possible for our limited sample of quasar candidates.

In order to provide further information, we compared the survey results with those obtained from numerical simulations. Only rough estimates can be made. Quasar populations mimicking the observed large-scale redshift distribution were synthesized and some percentage (a parameter) of the quasars were paired with a separation inferior to 10 h^{-1} Mpc. We admitted that our final sample was containing 40 per cent contaminants; we also included the redshift errors by scrambling the values with the appropriate Gaussian curve and by rendering the scale discrete. Some 30 per cent of the lines were assumed as being misidentified as Lyα (see e.g. Clowes *et al.* 1987). The CFA statistic $w_{\mathrm{data/data}}$ has been computed; from its distribution over the simulations, we conclude that the value observed here can only be reached if we admit that, at least, some 10 to 25 per cent of the quasars are paired. The extreme value of 10 per cent is not in disagreement with the 12 per cent reported by Shanks *et al.* (1988) but this percentage is in general quite large (compared, for example, to the results of Clowes *et al.* 1987). Two effects could be causing the discrepancy: either our sample contains more than 60 per cent of quasars, or the contaminants conspire to mimic clustering. Both effects could not have been included *a priori* in our simulations.

If we combine our results, suggesting that the CFA is more sensitive than the PSA, with the statement by Drinkwater (1988) that the difference in sensitivity can reach a factor of about 2, we should not be surprised at the non-detection of any effect by the GPSA.

4 THE RELATIVE POSITIONS OF THE CANDIDATES WITH RESPECT TO NGC 520

The field around NGC 520 is of particular interest since Arp & Duhalde (1985) have pointed out several anomalies concerning the distribution of quasars. The first main anomaly they reported is an excess of quasars within a few tenths of a degree from the galaxy NGC 520; the second one is the presence of a strong anisotropy: a NE–SW alignment of bright quasars across this galaxy. In order to contribute to the test of their reality, we decided to search for these anomalies in our sample of quasar candidates.

Counts of candidates were made in 2D concentric rings around the galaxy; the counts were corrected for edge effects. In fact, this technique is similar to that used for the computation of the CFA in Section 3.1. No significant deviation from randomness has been detected for any distance up to 1°.5. In particular, within half a degree of NGC 520, we find seven quasar candidates whereas the expected number is 5.5. The difference is not significant at all, as confirmed by our simulations. This result is in good agreement with the large-scale uniformity reported in Section 3.1. Our sample is, of course, quite different from that of Arp & Duhalde (1985) but, as it had been selected in a spatially homogeneous way, any deviation of the order of that claimed by Arp & Duhalde (1985) should have been detected if it had belonged to the parent population. Recently, Boyle, Fong & Shanks (1988) have investigated the general correlation of UVX quasars with galaxies. They find no positive correlation but some evidence for an anticorrelation, for scales less than 4 arcmin, between quasars and galaxies belonging to clusters. Although the population of galaxies they used cannot be directly related to the single object NGC 520, their results are not in disagreement with ours.

We have also analysed the distribution of the position angles of our quasar candidates with respect to NGC 520. The distribution is clearly not uniform; this is due to two facts: NGC 520 is not located at the centre of the field and the field is a square. We have generated several thousands of synthetic populations of 175 individuals. For each, the distribution of the position angles can be deduced. On the basis of these simulations, we have computed the mean distribution and the relevant standard deviation under the null-hypothesis of randomness. The observed distribution never deviates from the computed one by more than 2.2 standard deviations, suggesting that there is no privileged direction around NGC 520 with either an excess or a depletion of quasar candidates. The simulated mean cumulative distribution function of the position angles is given in Fig. 4 along with the observed (sample) one. The agreement is good and could be tested through, for example, the largest deviation

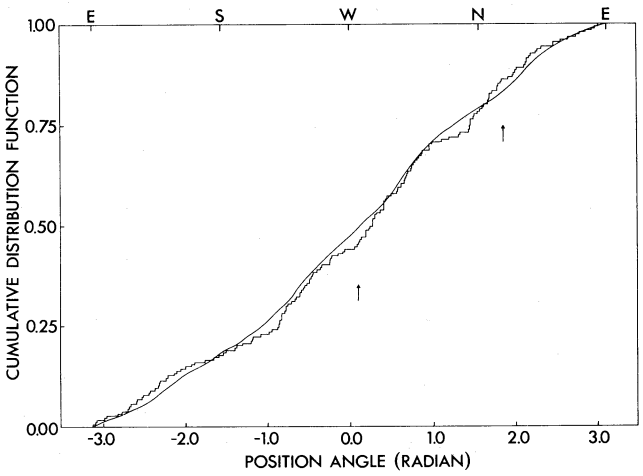

Figure 4. Expected (continuous line) and observed (staircase line) cumulative distribution functions (cdf) of the position angles of the 175 quasar candidates with respect to NGC 520. The cumulation arbitrarily starts at the east of the galaxy (defined to correspond to PA$= -\pi$) and is performed counterclockwise (ESWN). The largest deviation of each type (expected cdf dominating the observed one and the reverse) is indicated by an arrow (see text in Section 4 for details).

observed. Such an approach is typical of the well-known Kolmogorov–Smirnov test. Arrows in Fig. 4 indicate the two largest deviations: one for which the observed function dominates the simulated function (right-hand arrow) and the other for which the reverse is true (left-hand arrow). These deviations correspond to the usual one-sided Kolmogorov–Smirnov statistics D^+_{175} and D^-_{175}, respectively. We thus have $D^+_{175} = 0.031$ and $|D^-_{175}| = 0.047$. However, the position angle has the nature of a circular statistic, and therefore the starting point of the cumulation is completely arbitrary. The Kolmogorov–Smirnov statistic being highly dependent on this starting point, the test in the usual form is not valid. Kuiper (1960) has shown that the sum of the two one-sided statistics is independent of the above mentioned point and has introduced the statistic

$$V_n = D^+_n + |D^-_n|.$$

In our case, we have $V_{175} = 0.078$ and a comparison with the probability formula given by Kuiper (1960) indicates that the adopted null-hypothesis is not rejected at all.

In order to strengthen our conclusions, the high-grade sample has also been searched for alignments. We used two statistical methods. The first one, devised by Kendall (1984), consists in investigating the shape-space the points of which represent the shapes of not totally degenerate triads in a 2D plane. All the objects in the field are taken three by three; each of such triangles can be characterized by its shape when any translation, dilatation or rotation is quotiented out. Kendall (1984) proved that the natural shape-space of labelled triangles is isometric with a 2D sphere (the surface of a 3D sphere). If we further neglect the labelling of the vertices, the abovementioned sphere is split into six equivalent lunes. If we finally neglect the distinction between a shape and its reflexion, we have to deal with a half-lune; the latter is named the spherical blackboard by Kendall (1984). Plate 1 gives an 'opened out' cylindrical projection of the spherical blackboard. Vertex N corresponds to the locus of equilateral triangles whereas the arc LM is the locus of triangles degenerated into a single line (alignments!). Arc NM is the locus of isosceles triangles for which one of the vertices is tending towards the centre of the opposite edge whereas arc NL is the locus of isosceles triangles degenerating into a single line by the merge of two vertices. We refer the reader to fig. 2 of Kendall (1984) for further details. The advantage of the method is that, if the triangles in the plane are completely independent, the density of the shape points over the spherical blackboard is uniform. The realization corresponding to our 175 quasar candidates is included in the spherical blackboard of Plate 1. The density is a little higher towards vertices N and L, and lower towards vertex M. This is a consequence of the fact that our field is not the whole 2D plane but instead is a square with limits. The overdensity towards the vertex L is not reaching it, indicating some lack of close pairs: a result in good agreement with our conclusions of Section 3.1. The important result here is that no relative enhancement of the density of the shape points is visible along the arc LM, i.e. no tendency towards alignments is present. Application of the relevant test of Kendall (1984) confirms the absence of any excess of alignments.

The second statistical method we used for investigating potential alignments consists of a point-line transformation. The basic idea is simple: each point representing the position of an object is transformed into a line such that several aligned points will give rise to lines going through the same intersection point. In the space of the intersection points between the lines, an approximate alignment will correspond to a cluster: such a space can be studied using standard clustering methods. In particular, a statistic based on the minimum spanning tree edge-length distribution is sufficiently powerful (Gosset, Surdej & Swings 1987). An interesting property of this method is that the reciprocal transformation can be applied to the centroid of the outstanding clusters in order to reveal the possible alignments. The application of this method to the high-grade sample leads to the detection of no significant alignment, a conclusion similar to the one by Gosset *et al.* (1987) which was based on another data set.

Our present results thus disagree with the conclusions of Arp & Duhalde (1985). The main reason could be that the two samples are dissimilar: the selection techniques used and therefore the resulting redshift ranges are different. This remark, however, does not apply to the data set analysed by Gosset *et al.* (1987). Consequently, as both analyses disagree with the conclusions of Arp & Duhalde (1985) and as both samples were derived in an (as much as possible) homogeneous manner, we tend to attribute the discrepancy to the fact that Arp & Duhalde's (1985) sample was actually biased. This could happen for many reasons: for example, search for quasars in ill-defined regions, limits of the survey settled afterwards...

5 CONCLUSIONS

We have presented here the results of an objective-prism search for quasars in a field around the galaxy NGC 520. This is the first part of a project that aims at studying with such a complementary method a region already searched for by the U/B excess technique (Gosset *et al.* 1986; Swings *et al.* 1988). State-of-the-art automated detection methods (AQD; Clowes 1986a, b, 1988) have been used to derive a homogeneous sample of 175 high-grade quasar candidates. Accurate positions of the latter are given in Table 3.

The distribution of the selected objects has been analysed in detail. The 2D (α, δ) distribution of the quasar candidates exhibits two important features. The first one is the existence of a significant excess of objects at separations of about 20 arcmin. The second one is a tendency to exhibit anticorrelation on a scale of a few arcminutes. Although we have been able to detect the effect of the systematic discarding of overlapping spectra, we can conclude that this effect contributes little to the observed anticorrelation.

We have tentatively derived redshifts for the candidates of our sample on the basis of their objective-prism spectra. This information has been used in order to study the 3D (spatial) distribution of the candidates. Large-scale inhomogeneities associated with the non-uniformity of the distribution of the observed provisional redshifts are present. In addition, a tendency to cluster predominantly due to the formation of pairs is detected at a typical scale of about $10\ h^{-1}$ Mpc (significance level of 0.04). For several reasons, the latter statement is to be noted with great care. First, the significance level is not low enough to permit secure rejection of the null-hypothesis. Secondly, the reported clustering is due to a very small number of objects and some errors are expected to

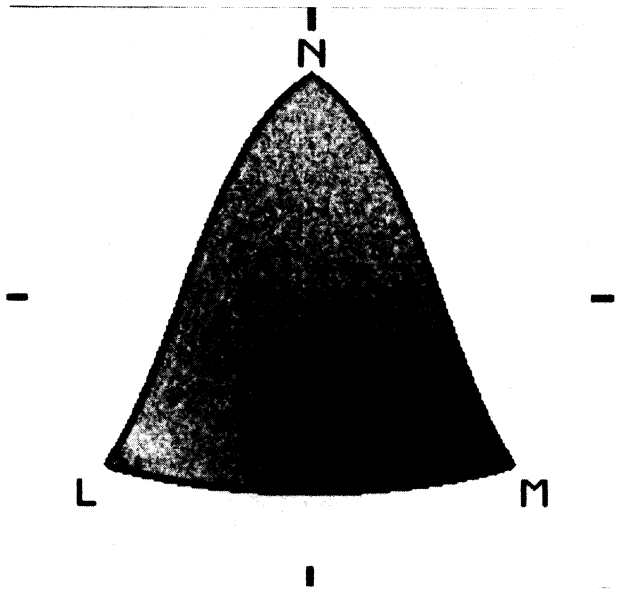

Plate 1. Projection of the basic region of the shape-space (spherical blackboard of Kendall 1984). Each point of this space corresponds to a particular shape of a triangle in the plane. All the possible triangles formed by the 175 quasar candidates have been included in this diagram, and the relative density of the shape points is given on a grey-scale. The local density is proportional to the local brightness. Note the absence of a relative enhancement of density along the LM arc which is the locus of triangles degenerated into a single line (i.e. alignments).

[Facing p. 80]

exist in the determination of the redshifts (precisely at a scale of about 10 h^{-1} Mpc); in particular, their discrete nature, due to an observational artefact, must be kept in mind. Thirdly, it could also be that some of the high-grade quasar candidates actually consist of stars.

We have also investigated the possible relations between our sample of quasar candidates and NGC 520: our sample exhibits no visible dependence with respect to this galaxy.

The next natural steps in our investigation will be to acquire and reduce another objective-prism plate with the dispersion rotated by 90° and to perform a spectroscopic identification of all the high-grade quasar candidates.

ACKNOWLEDGMENTS

The authors acknowledge UKSTU and ESO for the plates and COSMOS for the measurements. Some of the data processing was performed on the UK STARLINK computers. EG would like to thank the staff of ROE for their hospitality during a stay in 1984.

NOTE ADDED IN PROOF

Some of the candidates listed in Table 3 are in fact also present in the *U*/*B* excess sample: the corresponding spectroscopic identification confirms that objects 7, 45, 55, 88, 103, 110 and 112 are indeed quasars. More details will be published in the paper dealing with the *U*/*B* survey.

REFERENCES

Arp, H. C., 1981. *Astrophys. J.*, **250,** 31.
Arp, H. C., 1983. In: *Quasars and Gravitational Lenses, 24th Liège Astrophysical Colloq.*, p. 307, ed. Swings, J. P.
Arp, H. C. & Duhalde, O., 1985. *Publs astr. Soc. Pacif.*, **97,** 1149.
Arp, H. C. & Surdej, J., 1982. *Astr. Astrophys.*, **109,** 101.
Boyle, B. J., Fong, R. & Shanks, T., 1988. *Mon. Not. R. astr. Soc.*, **231,** 897.
Clowes, R. G., 1986a. *Mon. Not. R. astr. Soc.*, **218,** 139.
Clowes, R. G., 1986b. *Mitt. astr. Ges.*, **67,** 174.
Clowes, R. G., 1988. *Astr. Soc. Pacif. Conf. Ser., Proc. Workshop on Optical Surveys for Quasars, Vol. 2,* p. 75, eds Osmer, P. S., Porter, A. C., Green, R. F. & Foltz, C. B.
Clowes, R. G. & Savage, A., 1983. *Mon. Not. R. astr. Soc.*, **204,** 365.
Clowes, R. G., Iovino, A. & Shaver, P., 1987. *Mon. Not. R. astr. Soc.*, **227,** 921.
Drinkwater, M. J., 1986. In: *Quasars, IAU Symp. No. 119,* p. 503, eds Swarup, G. & Kapahi, V. K., Reidel, Dordrecht.
Drinkwater, M. J., 1988. *Mon. Not. R. astr. Soc.*, **235,** 1111.
Fall, S. M., 1979. *Rev. mod. Phys.*, **51,** 21.
Gosset, E., 1987a. *Astr. Astrophys.*, **188,** 258.
Gosset, E., 1987b. *Analyse de nuages de points.* Applications astronomiques et étude de la distribution des quasars, *Thèse de Doctorat*, Université de Liège.
Gosset, E. & Louis, B., 1986. *Astrophys. Space Sci.*, **120,** 263.
Gosset, E., Surdej, J. & Swings, J. P., 1986. In: *Quasars, IAU Symp. No. 119,* p. 45, eds Swarup, G. & Kapahi, V. K., Reidel Dordrecht.
Gosset, E., Surdej, J. & Swings, J. P., 1987. In: *Observational Cosmology, IAU Symp. No. 124,* p. 499, eds Hewitt, A., Burbidge, G. & Fang, L. Z., Reidel, Dordrecht.
Gosset, E., Surdej, J. & Swings, J. P., 1988. *Astr. Soc. Pacif. Conf. Ser., Proc. Workshop on Optical Surveys for Quasars, Vol. 2,* p. 281, eds Osmer, P. S., Porter, A. C., Green, R. F. & Foltz, C. B.
Iovino, A. & Shaver, P. A., 1988. *Astrophys. J.*, **330,** L13.
Kendall, D. G., 1984. *Bull. London Math. Soc.*, **16,** 81.
Kruszewski, A., 1988. *Acta Astr.*, **38,** 155.
Kruszewski, A., 1990. *Astrophys. J.*, submitted.
Kuiper, N. H., 1960. *K. Nederlandse Akad. Wetensch. Proc.*, **A63,** 38.
MacGillivray, H. T. & Stobie, R. S., 1984. *Vistas Astr.*, **27,** 433.
Oort, J. H., 1981. *Astr. Astrophys.*, **94,** 359.
Oort, J. H., 1983. In: *Quasars and Gravitational Lenses, 24th Liège Astrophysical Colloq.*, p. 301, ed. Swings, J. P.
Oort, J. H., Arp, H. C. & de Ruiter, H., 1981. *Astr. Astrophys.*, **95,** 7.
Peacock, J. A., 1983. *Mon. Not. R. astr. Soc.*, **202,** 615.
Shanks, T., Boyle, B. J. & Peterson, B. A., 1988. *Astr. Soc. Pacif. Conf. Ser., Proc. Workshop on Optical Surveys for Quasars, Vol. 2,* p. 244, eds Osmer, P. S., Porter, A. C., Green, R. F. & Foltz, C. B.
Sharp, N. A., 1979. *Astr. Astrophys.*, **74,** 308.
Surdej, J., Swings, J. P., Arp, H. C. & Barbier, R., 1982. *Astr. Astrophys.*, **114,** 182.
Swings, J. P., Surdej, J. & Gosset, E., 1988. *Astr. Soc. Pacif. Conf. Ser., Proc. Workshop on Optical Surveys for Quasars, Vol. 2,* p. 61, eds Osmer, P. S., Porter, A. C., Green, R. F. & Foltz, C. B.
Webster, A. S., 1976a. *Mon. Not. R. astr. Soc.*, **175,** 61.
Webster, A. S., 1976b. *Mon. Not. R. astr. Soc.*, **175,** 71.